Available online at www.sciencedirect.com
SCIENCE DIRECT®

Journal of the European Ceramic Society 24 (2004) 2203–2213

www.elsevier.com/locate/jeurceramsoc

Electrostatic atomisation of a ceramic suspension

S.N. Jayasinghe, M.J. Edirisinghe*

Department of Materials, Queen Mary, University of London, Mile End Road, London E1 4NS, UK

Received 28 February 2003; received in revised form 11 July 2003; accepted 19 July 2003

Abstract

An alumina suspension, containing ~20 vol.% of powder was pumped through a needle held at a high voltage, with respect to a point-like ground electrode, and subjected to electrostatic atomisation. The flow rate and voltage was varied between 10^{-9} and 10^{-8} m^3 s^{-1}, and 5 and 12 kV, respectively and the mode of atomisation observed was recorded to construct mode selection (M-S) maps. In the stable cone-jet mode, the jet diameter was measured as a function of flow rate and applied voltage. Alumina relics obtained in the stable cone-jet mode regime were collected and studied by optical microscopy to establish the conditions which generated the finest relics.

Keywords: Electrostatic atomisation; Cone-jet mode; Suspension; Relics

1. Introduction

Electrostatic atomisation, also known as electrospraying, refers to a process where a liquid jet breaks into a spray (droplets) under the influence of an electrical field.[1,2] The process is influenced by many parameters[3,4] such as liquid properties (mainly electrical conductivity and viscosity), liquid flow rate and the applied voltage. It can take place in many spray modes and these are described in detail in the aerosol science litreture.[3,4] However, the ceramics community are not familiar with the classification of spray modes and therefore a brief description of these are given below. The spray modes observed in this work are also illustrated with figures in Section 3.

Micro-dripping tends to occur at low liquid flow rates and produces a narrow size distribution of droplets with a low droplet production frequency. In this mode, when the electrical forces acting on the hanging droplet overcome the surface tension forces, a small droplet is ejected. Once this droplet is ejected the liquid at the exit of the needle relaxes and the process is repeated with the growth of another drop.[5]

Spindle and multi-spindle modes are observed at higher flow rates and are accompanied by higher electrical forces. In these modes a cone is formed at the exit of the needle with a jet emerging from its apex. The jet breaks up in to small droplets, which are highly charged. Subsequently, the cone and jet relax, and the process is repeated. However, in the case of the multi-spindle mode, after relaxation, another cone and jet emerge from the opposite side to the first formed cone and jet.[6] These two modes produce broad size distributions of droplets.

When a near-monodisperse droplet size distribution is required, the stable cone-jet mode is a pre-requisite.[2] This mode of atomisation occurs when the electric field strength and the surface tension of the liquid are equal. The intermittent cone-jet mode, which generally lies between the spindle/multi-spindle and the stable cone-jet mode is similar to the cone-jet mode but is unstable. Also, the intermittent (unstable) cone-jet mode and the spindle mode can appear to be similar but the main difference between these two modes is that in the latter, the jet appears to skew and later fragments into droplets.[7]

With increasing applied voltage the depth of the liquid cone in the stable cone-jet mode decreases. Thus, at a critical applied voltage the cone is too small for the needle. When this occurs the cone moves from the centre of the needle towards the edge of the needle and when the applied voltage is increased further a second

* Corresponding author. Tel.: +44-20-7882-7767; fax: +44-20-8981-9804.
E-mail address: m.j.edirisinghe@qmul.ac.uk (M.J. Edirisinghe).

0955-2219/$ - see front matter © 2003 Elsevier Ltd. All rights reserved.
doi:10.1016/j.jeurceramsoc.2003.07.001

Table 1
Bead mill operating conditions

Variable	Details
Tip Speed	14 ms^{-1}
Type of beads	0.5 mm diameter yttria stabilized zirconia
Volume of beads in chamber	216 ml (80% of capacity)
Pump flow rate	0.5 ml s^{-1}
Milling temperature	40 °C (Maximum)
Stirrer motor current	0.2 A

cone is formed. If increase in applied voltage is continued more cones appear with the base of the cones attached to one another and the spraying mode becomes multi-jet.[8]

If the flow rate is relatively high ($\sim 10^{-3}$ m^3 s^{-1}), the liquid has a large enough kinetic energy, which cannot be compensated by surface tension. Thus, the liquid simply becomes a jet and breaks into droplets. This is the simple-jet mode.[9] If the electric field around the simple jet is increased, this can cause a radial electrical stress which overcomes surface tension and smaller jets begin to emerge from the main jet (appearance of a "fir tree-like" pattern). These small jets break up to produce a polydisperse droplet distribution and this is called the ramified jet mode.[3]

Electrostatic atomisation of ceramic suspensions in the stable cone-jet mode can give near-monodisperse droplet relics of a few μm in size,[10] much finer than those produced by ink-jet printing, and this is the reason for this mode being preferred in the present investigation.

The work carried out by Kim and Turnbull,[11] Chen et al.,[12] De la Mora and Loscertales,[13,14] Ganan-Calvo et al.,[15] and Hartman et al.[16–19] show that liquid properties, notably, dc electrical conductivity, viscosity, surface tension, relative permittivity and density, and two process parameters, namely applied voltage and flow rate, play a crucial role in achieving cone-jet mode electrostatic atomisation. If the dc electrical conductivity is too low ($< 10^{-10}$ S m^{-1}), the liquid cannot be sprayed in the cone-jet mode. The relative permittivity determines polarization in the liquid and in essence reduces the electric field within it making the attainment of the

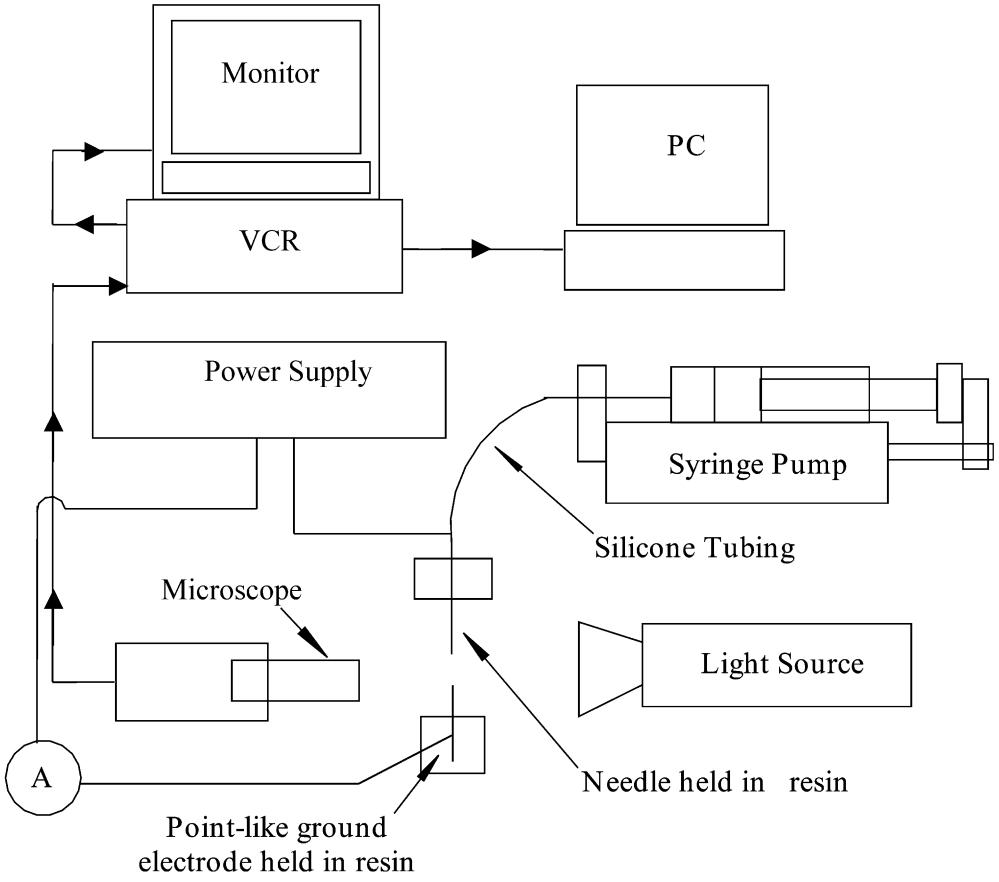

Fig. 1. Schematic diagram of electrostatic atomization apparatus used in the experiments.

cone-jet mode more difficult. Viscosity influences the jet break-up process and as a result has a significant effect on the size of droplets produced.[20] However, in most cases, the influence of viscosity on the droplet size is not considered since low viscosities of ~100 mPa s have been used. For the formation of a stable cone-jet, the surface tension must be overcome by the electric stresses. However, Ganan-Calvo et al.[15] show that the droplet size is independent of the surface tension for liquids which are highly conductive (1.3×10^{-3} S m^{-1}). Increase in liquid density decreases the minimum flow rate required for cone-jet mode electrostatic atomisation.[19] The scaling laws presented by Ganan-Calvo et al.[15] neglected density but Hartman et al.[19] have shown that density has an influence on droplet generation as it affects jet break-up.

If the applied voltage, which effects the magnitude of the electric field strength, is too low (~4 kV), then the spraying process is microdripping, spindle or unstable cone-jet mode but if it is too high (~11 kV), then spraying occurs in rim-emission or multiple-jet mode.[6,16] If the flow rate is low ($\sim10^{-15}$ m^3 s^{-1}) the

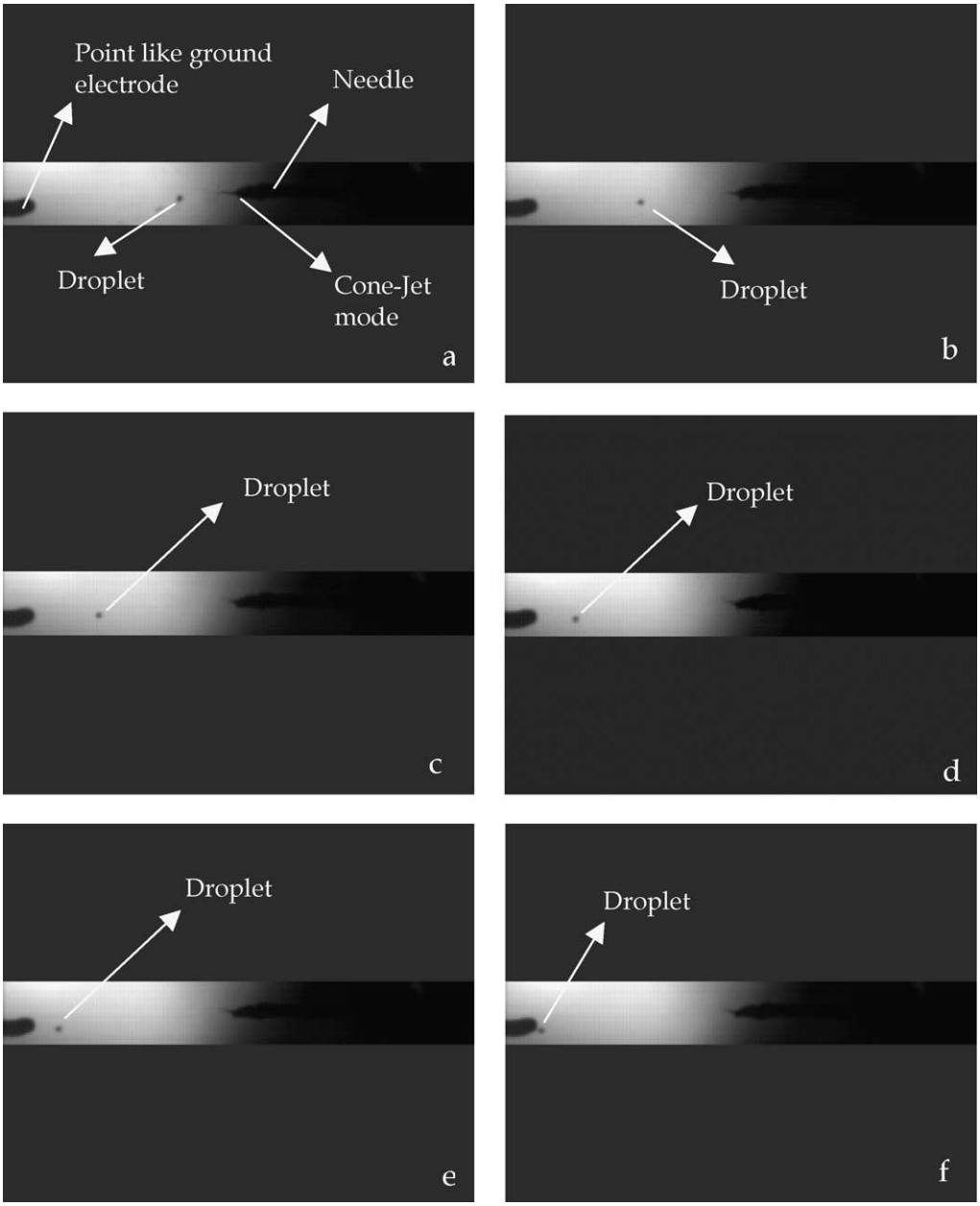

Fig. 2. Sequence a–f shows a droplet of the suspension moving from the exit of the needle and towards the point-like ground electrode. The Kodak EktaPro camera system was used to capture these images.

Table 2
Composition and properties of the milled alumina ink. Properties of the ethanol used in this investigation are also given

Alumina wt.%	vol%	Ethanol wt.%	EFKA 401 wt.%	Density kg m^{-3}	Viscosity mPa s	Surface tension mN m^{-1}	Electrical conductivity S m^{-1}	Relative permittivity
56.5	20.6	43.0	0.5	1413	1420	64	0.43×10^{-4}	54
Ethanol				790	1320	23	3.23×10^{-4}	26

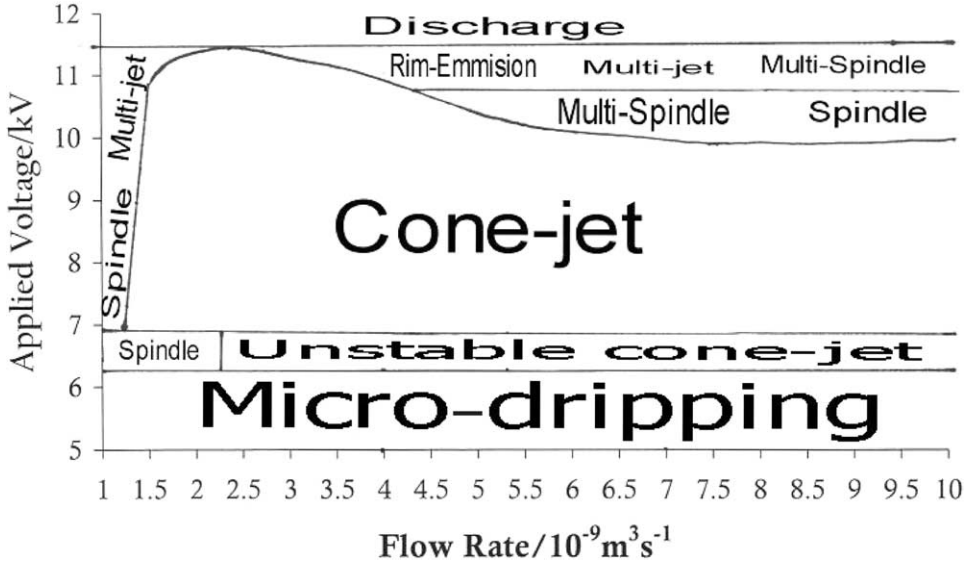

Fig. 3. M-S for the suspension in the flow rate regime 10^{-9}–10^{-8} m^3 s^{-1}. In some regions several modes were observed within a flow rate range and are stated separated by a slash.

spraying process is unstable because the liquid cone relaxes to a droplet shape periodically. Above a minimum flow rate, droplet generation stabilises and the size distribution of the droplets narrows. However, if the flow rate is increased above a critical value, then the droplet size distribution becomes more polydisperse and the process becomes more unstable. Ganan-Calvo et al.[15] and Rosell-Llompart et al.[21] have shown that the minimum flow rate is dependent on electrical conductivity and surface tension.

According to the literature, the alumina suspension used in this work contains the highest filler loading processed by a jet-based route. Its key properties, which affect electrostatic atomisation, were measured before subjecting it to electrospraying. M-S maps were constructed for this suspension in the flow rate and applied voltage regime of 10^{-9}–10^{-8} m^3 s^{-1} and 5–12 kV, respectively. The importance of varying the applied voltage and flow rate to control the jet diameter and relic/droplet size generated is demonstrated.

2. Experimental details

2.1. Materials

Near mono-disperse A16.SG alumina (3987 kg m^{-3}, supplied by ALCOA, Ludwigshafen, Germany) containing 0.5 μm particles was used. GPR grade ethanol (790 kg/m^3, supplied by BDH Laboratory Supplies, UK) was used as the liquid medium together with 0.5 wt.% of dispersant (Efka 401, 950 kg/m^3, supplied by Efka Chemicals, The Netherlands).

2.2. Mixing

Measured quantities of ethanol and Efka 401 dispersant were mixed into a beaker and stirred manually. Subsequently, alumina powder was added to the ethanol-Efka mixture and stirring was continued. Finally, the suspension was put through a high-energy bead mill (Glen Creston Dyno-mill, Type KDL A, Stanmore, UK). The operating details of the mill are shown in

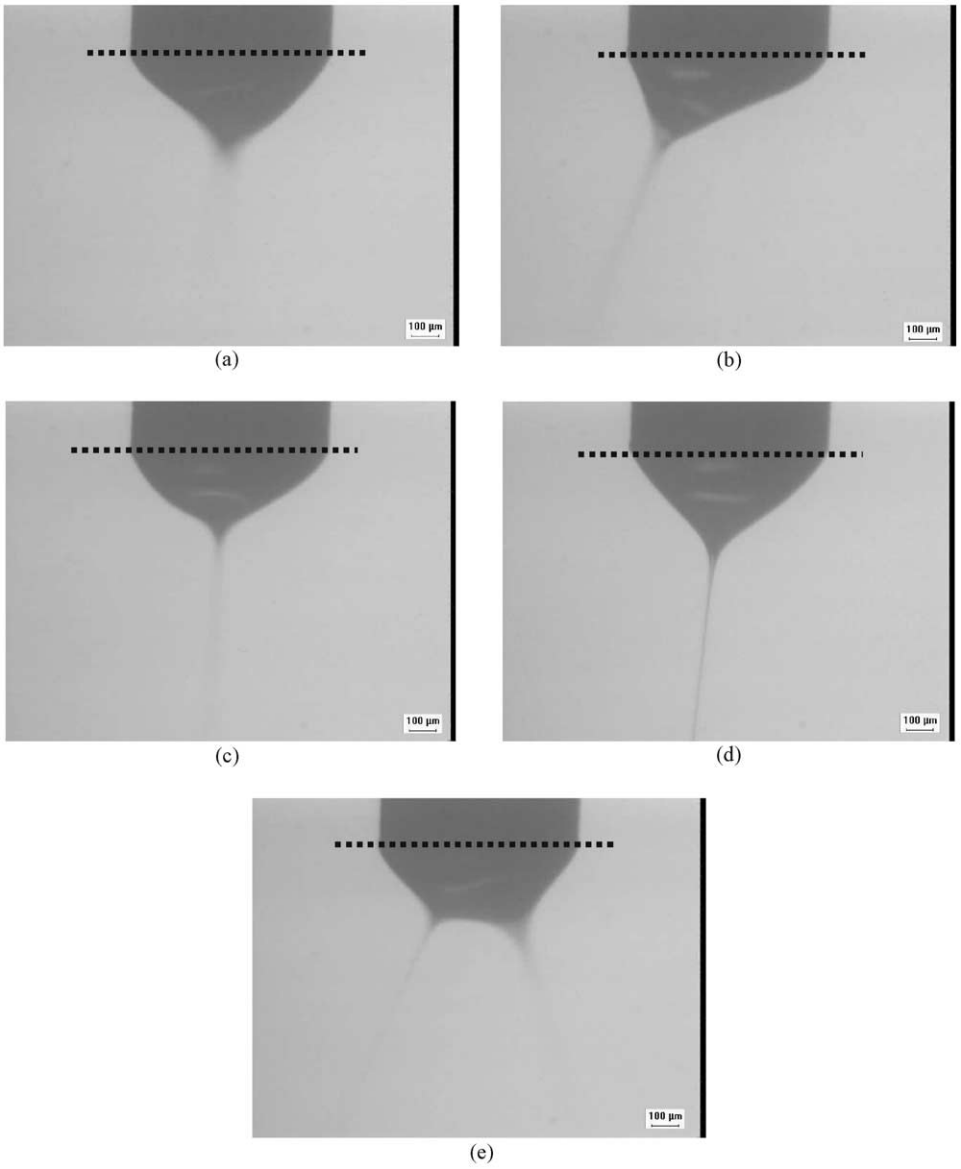

Fig. 4. Atomization of the ceramic suspension in (a) micro-dripping, (b) spindle, (c) unstable cone-jet, (d) stable cone-jet and (e) multi-spindle modes. The dotted line represents the exit of the needle.

Table 1. The suspension was passed through the mill five times and on each occasion the output was collected in a fresh container. Throughout the milling process the temperature was maintained <40 °C. The milled suspension was kept on rollers and agitated until required for electrostatic atomisation.

2.3. Suspension characterisation

The alumina content of the suspension was determined by loss-on-ignition by heating to 600 °C. The density was measured using the well-established density bottle method. Suspension viscosity was measured using a U-tube viscometer. The viscometer was immersed in a water bath maintained at 25 °C. DC conductivity and relative permittivity were measured using an appropriate glass cell having a known area/distance between electrodes (7.27×10^{-3} m and 0.26×10^{-3} m the case of the conductivity and permittivity, respectively). The surface tension was measured using the well-known Du Nouy ring method. Ethanol was used to calibrate the density, viscosity, dc conductivity, permittivity and surface tension measurements.

2.4. Sedimentation behaviour

A pyrex test tube was calibrated for volume against height. The suspension was poured into the tube, sealed and left undisturbed. The volume of sedimentation was recorded as a function of time.

2.4.1. Electrostatic atomisation

Electrospraying was performed using a stainless steel needle having a normal edged exit (90° to the needle axis). The inner and outer diameter of the needle was 0.2 and 0.5 mm, respectively). It was held in epoxy resin, 6 mm above a point-like (diameter ~0.13 mm) ground electrode also held in epoxy resin and kept inline with the needle as shown in Fig. 1.

The needle inlet was connected to a syringe mounted on a Semat A99FMZ pump (Semat International Ltd., St. Albans, UK) using silicone rubber tubing. The flow rates were varied by either changing the cross-section area of the syringe or by using the rate selector switch in the pump. The flow rate was calibrated over long (60, 180, 300 and 600 s) and short (1, 3, 5 and 10 s) periods of time, as flow rate consistency is an important factor in electrostatic atomisation. A Glassman FC30 high voltage power supply (Glassman Europe Ltd., Tadley, UK), which was capable of applying up to 30 kV, was used to apply voltage to the needle.

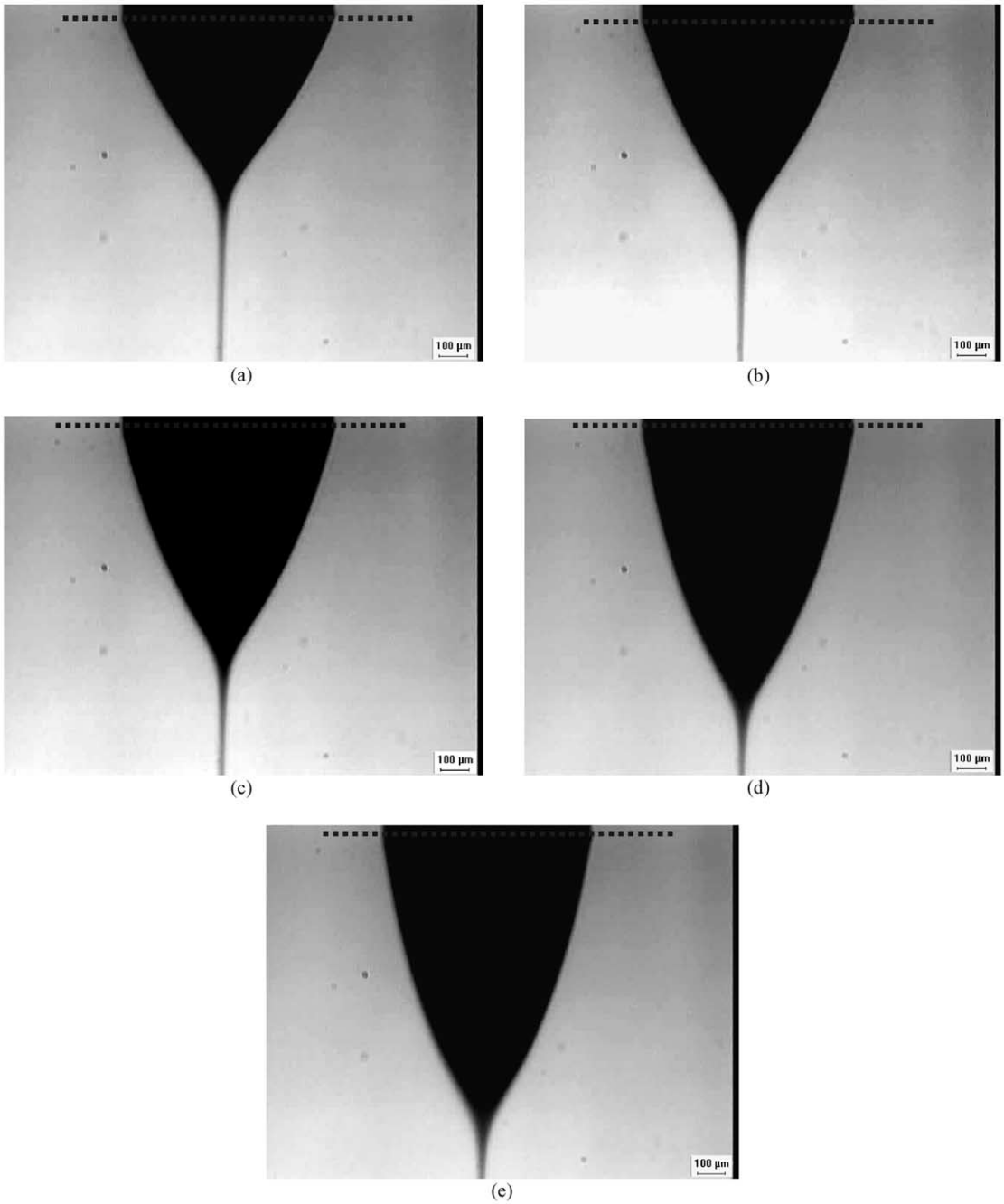

Fig. 5. Variation in cone shape with increasing flow rate ($\times 10^{-9}$ m^3 s^{-1}): (a) 2, (b) 4, (c) 6, (d) 8 and (e) 10 at a constant applied voltage of 8 kV. The dotted line represents the exit of the needle.

A microscope was used in conjunction with a CCTV camera (WAT-502A Watec Co. Ltd., Kanagawa, Japan), a monitor, a computer and a video to record the electrostatic atomisation process, in particular in the vicinity of the needle. The jet diameter was measured using the information recorded. A high-speed camera (Kodak EktaPro, EM motion Analyser/Model 1012) was used to capture droplet trajectories as they emerged from the jet. This camera was capable of capturing 12000 frames s^{-1}.

2.5. Relic characterisation

The relics of the droplets were studied directly after deposition on a polyester coated 75×25 mm rectangular substrate (supplied by Autotype International Ltd., Wantage, UK). Relic sizes were measured by optical microscopy using Image-Pro Plus software (Media Cybernetics, L.P. Del Mar, CA, USA). The entire substrate was traversed under the microscope both length-wise and width-wise, taking care not to miss any relics.

3. Results and discussion

3.1. Needle and ground electrode

The shape and the wettability of the needle material can significantly influence the shape of the cone formed, the stability of the jet and the mode of atomisation.[8] Cloupeau and Prunet-Foch[5] also state that a change in wettability of the capillary causes liquid to accumulate at the exit of the needle, forming a meniscus over all or part of the perimeter of the needle. The liquid accumulated in this way periodically emits a jet, which can contain fine droplets and then finally detach as a large droplet.

The geometry of the ground electrode determines the trajectory of the droplets. A ring shaped ground electrode produces a conical spray with larger droplets segregated in the central regions and the finest droplets recirculate about the ring.[15,19] In contrast, a point-like ground electrode used in this work helped to focus most of the droplets, as shown in Fig. 2, although some scatter persists.[22] This has been used in innovating electrostatic atomisation printing (EAP)

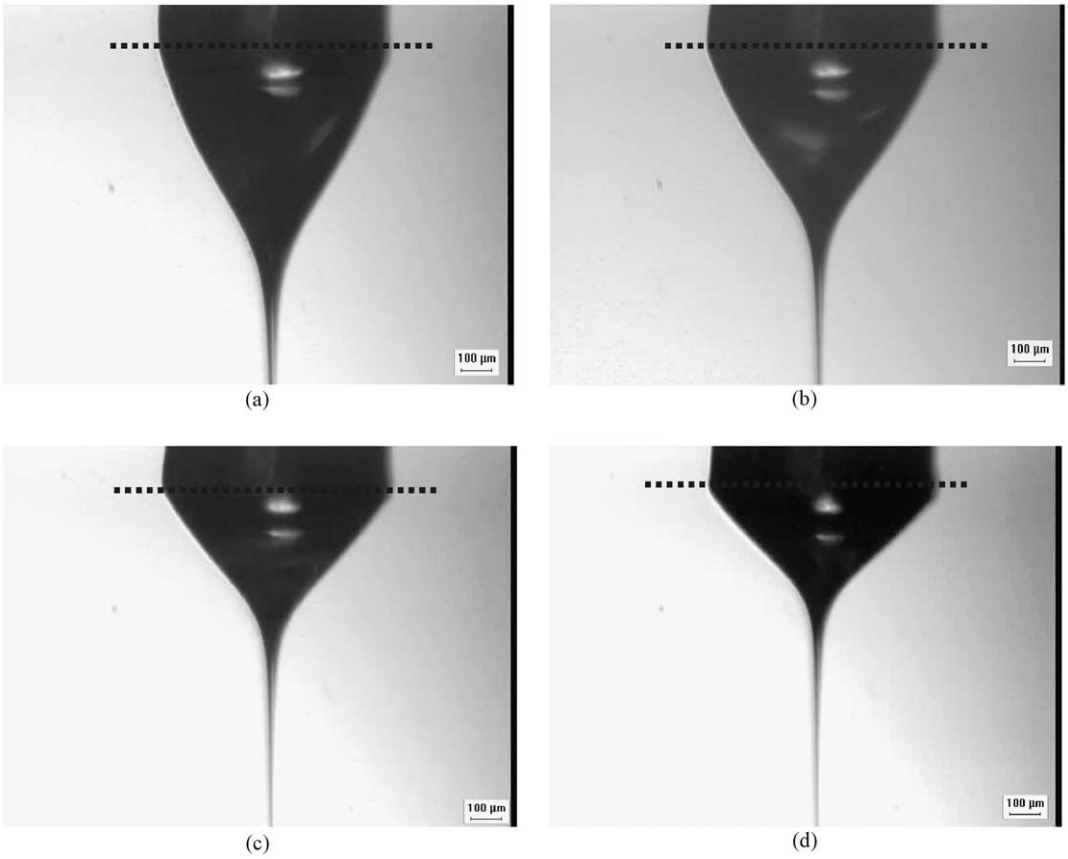

Fig. 6. Variation in cone shape with increasing applied voltage (kV): (a) 8, (b) 9, (c) 10 and (d) 11 at a constant flow rate of 1.67×10^{-9} m^3 s^{-1}. The dotted line represents the exit of the needle.

3.2. Suspension characteristics

Sedimentation in the first 10,800 s (3 h) was negligible. However, over 36×10^3 s (10 h) some, sedimentation was observed. Therefore, the suspension was mixed continuously on rollers until required for electrostatic atomisation. Composition and properties of the alumina suspension are given in Table 2. The properties of ethanol are also given in Table 2 for comparison. The major feature is the high viscosity, compared with previous electrostatic atomisation studies[13,18] using liquids with viscosities of <150 m Pa s.

According to Rosell-Llompart and de la Mora[21], in the cone-jet mode, the effect of viscosity on droplet size is dependent on the dimensionless parameter π_η given by:

$$\pi_\eta = \frac{\sqrt[3]{\gamma^2\rho\beta\varepsilon_0}}{\eta} \quad (1)$$

In Eq. (1), γ, ρ, β, ε_0, η are the surface tension, density, relative permittivity, permittivity of free space and viscosity, respectively. As indicated, η dominates the value of π_η compared with the other variables (γ, ρ and β). If π_η is $\gg1$ viscosity has no effect but if $\ll1$, the droplet size increases with increasing viscosity and moreover, a broader size distribution of droplets occur. Using data in Table 2, for the alumina suspension used in this work $\pi_\eta\ll1$ and therefore a significant effect of viscosity on the size of droplet relics generated can be expected. For this suspension, compared with ethanol, the electrical conductivity is low and the relative permittivity is high, both due to the addition of the alumina powder. Liquids with similar low electrical conductivities have been used in previous electrostatic atomisation studies and the stable cone-jet mode has been produced.[10,23]

3.3. Atomisation modes

A map showing the various modes of atomisation of the ceramic suspension as a function of flow rate and applied voltage is given in Fig. 3. At <6 kV, micro-dripping (Fig. 4a) was observed during the entire flow

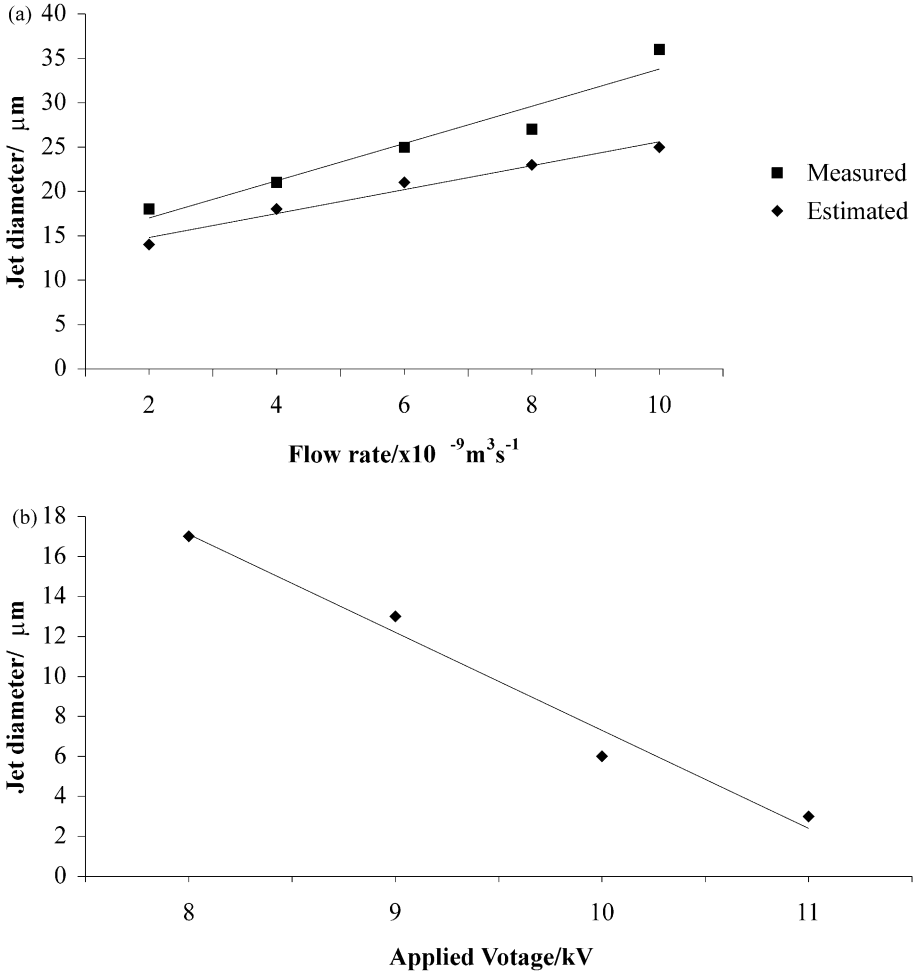

Fig. 7. Variation of jet diameter with (a) flow rate at a constant applied voltage of 8 kV and (b) applied voltage at a constant flow rate of 1.67×10^{-9} m^3 s^{-1}.

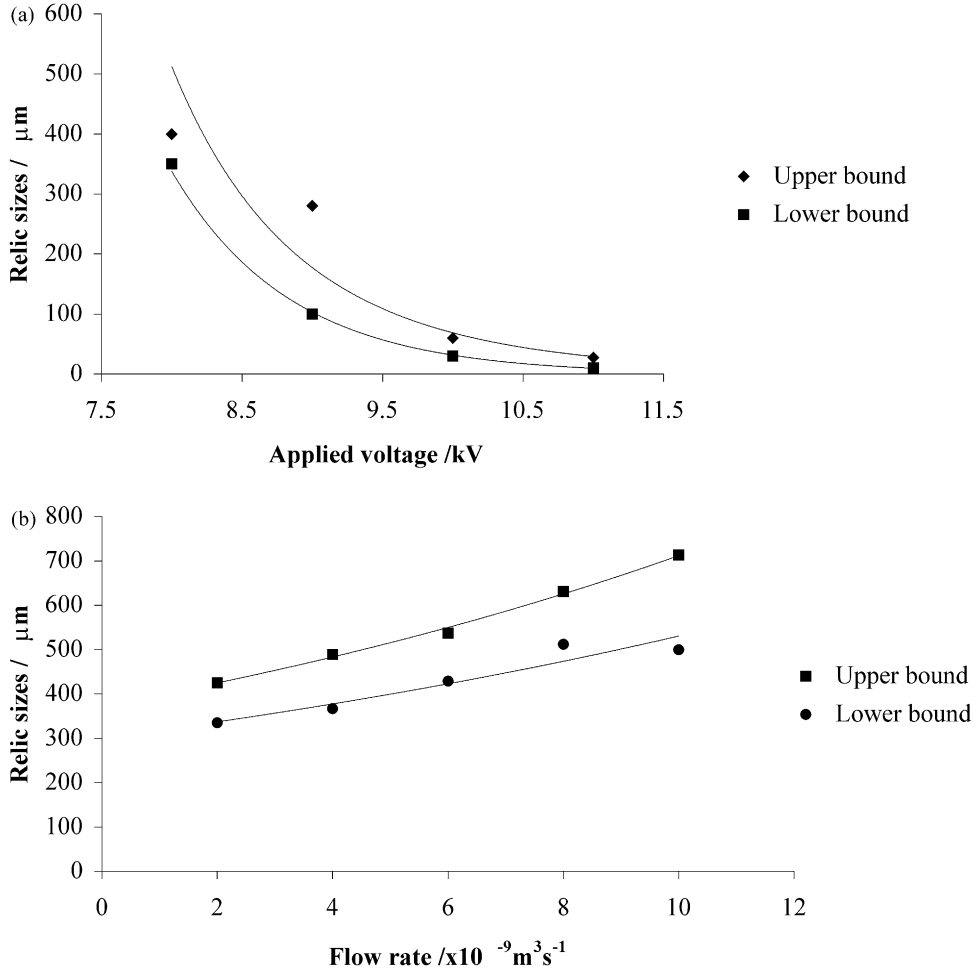

Fig. 8. Variation in relic size with (a) applied voltage at a constant flow rate of 1.67×10^{-9} m^3 s^{-1} and with (b) flow rate at a constant applied voltage of 8 kV.

rate regime investigated. Further increase in applied voltage upto 7 kV caused the mode to change to spindle (Fig. 4b) at low flow rates ($<2.25\times10^{-9}$ m^3 s^{-1}) and unstable cone-jet (Fig. 4c) at higher flow rates as shown in Fig. 3. Further increase in the applied voltage to between 7–10 kV resulted in producing the stable (steady) cone-jet mode (Fig. 4d) over the entire flow rate regime, except at very low flow rates of $\sim10^{-9}$ m^3 s^{-1}. The steady cone-jet mode was also achieved between $\sim$10 and 11.5 kV and flow rates between $\sim1.5\times10^{-9}$ and $\sim4.25\times10^{-9}$ m^3 s^{-1} but increasing the flow rate resulted in the mode changing mainly to the multi-spindle mode (Fig. 4e).

3.4. Cone depth, jet diameter and relic sizes

In the stable cone-jet mode, the cone and jet dimensions were measured using video recordings. The jet diameter was also estimated using theory.

The cone depth (distance from exit of needle to apex of cone) increased from 775 µm to 1050 µm on increasing flow rate from 2×10^{-9} m^3 s^{-1} to 10×10^{-9} m^3 s^{-1} as shown in Fig. 5. The increase in applied voltage had the opposite effect with the cone depth decreasing from 850 to 500 µm as a result of increasing the applied voltage from 8 to 11 kV (Fig. 6).

The viscous dimensionless parameter (δ_m) of this suspension can be calculated using:[15]

$$\delta_m = \sqrt[3]{\frac{\rho\varepsilon_0\gamma^2}{K\eta^3}} \tag{2}$$

K is the dc electrical conductivity. Using the values in Table 2 in Eq. (2) shows that δ_m for the suspension is <1 and therefore the jet diameter (d_j) in the stable cone-jet mode can be estimated by:[15]

$$d_j \approx \sqrt[3]{\frac{(\beta-1)^{\frac{1}{2}}Q\varepsilon_0}{K}} \tag{3}$$

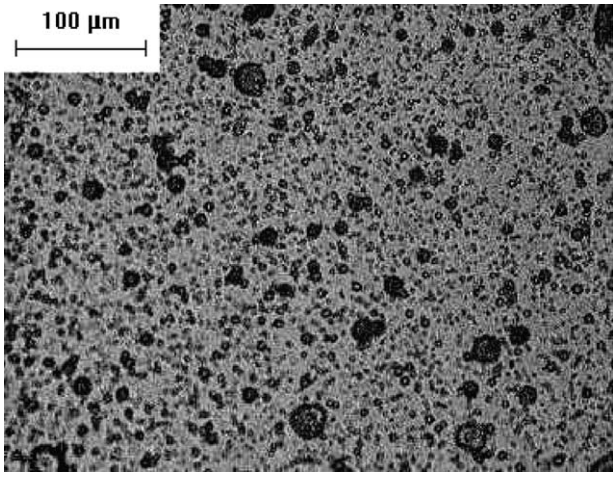

Fig. 9. Optical micrograph showing the finest alumina relics produced by electrostatic atomisation.

where Q is the flow rate. Using Eq. (3) and the values in Table 2 shows that d_j changes from 14 to 25 µm as the flow rate is increased from 2×10^{-9} m^3 s^{-1} to 10×10^{-9} m^3 s^{-1} (Fig. 7a). The increase in applied voltage from 8 kV to 11 kV also had a significant effect on the jet diameter, decreasing it from 17 to 3 µm (Fig. 7b). The d_j values calculated using Eq. (3) are also shown in Fig. 7a and it can be seen that these underestimate the jet diameter. This is not surprising as Eq. (3) does not directly take into account viscosity and applied voltage.

As shown in Fig. 7a and b, the jet diameter is inversely proportional to the applied voltage and directly proportional to the flow rate. This causes the alumina relic size to decrease with the former and increase with the latter (Fig. 8a and b). Therefore, these two vital process control parameter can be selected to achieve a minimum relic size. In the range investigated, an applied voltage of 11 kV and a flow rate of 1.67×10^{-9} m^3 s^{-1} gave the finest relics (Fig. 9).

4. Conclusions

A fully characterised suspension containing ~20 vol.% of ceramic powder has been subjected to electrostatic atomisation using a pointed ground electrode over a wide range of applied voltages and flow rates. The modes of electrostatic atomisation observed were recorded and a mode selection map of applied voltage-flow rate-mode was constructed. The electrostatic atomisation of the ceramic suspension was studied in detail in the cone-jet mode, elucidating the affect of the applied voltage and flow rate on cone and jet dimensions and droplet relic sizes. In this way, the conditions necessary for getting the finest relics were deduced; 11 kV and 1.67×10^{-9} m^3 s^{-1}, alumina relics <50 µm in size were deposited.

Acknowledgements

The authors wish to thank Queen Mary for awarding Dr. S.N. Jayasinghe a PhD scholarship, which enabled this work. We also gratefully acknowledge access to the EPSRC equipment loan facility and the help of Mr Adrian Walker (EPSRC/RAL) for the high-speed camera work presented in this paper.

References

1. Jaworek, A. and Krupa, A., Generation and disintegration of the precision mode of EHD spraying. *Journal of Aerosol Science*, 1996, **27**, 75–82.
2. Taylor, G. I., Disintegration of water droplets in an electric field. *Proceedings of the Royal Society (London)*, 1964, **280**, 383–397.
3. Jaworek, A. and Krupa, A., Classification of the modes of EHD spraying. *Journal of Aerosol Science*, 1999, **30**, 873–893.
4. Cloupeau, M. and Prunet-Foch, B., Electrostatic spraying of liquids: main functional modes. *Journal of Electrostatics*, 1990, **25**, 165–184.
5. Cloupeau, M. and Prunet-Foch, B., Electrostatic spraying of liquids in the cone-jet mode. *Journal of Electrostatics*, 1989, **22**, 135–159.
6. Luttgens, U., Dulcks, Th. and Rollgen, F. W., Field induced disintegration of glycerol solutions under vacuum and atmospheric pressure conditions studied by optical microscopy and mass spectrometry. *Surface Science*, 1992, **266**, 197–203.
7. Tang, K. and Gomez, A., Monodispersity electrosprays of low electric conductivity liquids in the cone-jet mode. *Journal of Colloid and Interface Science*, 1996, **184**, 500–511.
8. Cloupeau, M. and Prunet-Foch, B., Recipes for use of EHD spraying in the cone-jet mode and notes on corona discharge effects. *Journal of Aerosol Science*, 1994, **25**, 1143–1157.
9. Bailey, A. G., *Electrostatic Spraying of Liquids*. Research Studies Press, 1988.
10. Teng, W. D., Huneiti, Z. A., Machowski, W., Evans, J. R. G., Edirisinghe, M. J. and Balachandran, W., Towards particle-by-particle deposition of ceramics using electrostatic atomisation. *Journal of Materials Science Letters*, 1997, **16**, 1017–1019.
11. Kim, K. and Turnbull, R. J., Generation of charged drops of insulating liquids by electrostatic spraying. *Journal of Applied Physics*, 1976, **47**, 1964–1969.
12. Chen, D.-R., Pui, D. Y. and Kaufman, S. L., Electrospraying of conducting liquids for monodisperse aerosol generation in the 4nm to 1.8mm diameter range. *Journal of Aerosol Science*, 1995, **26**, 963–977.
13. Fernandez de la Mora, J. and Loscertales, I. G., The current emitted by highly conducting Taylor cones. *Journal of Fluid Mechanics*, 1994, **260**, 155–184.
14. Fernandez de la Mora, J., Navascues, J., Fernandez, F. and Rosell-Llompart, J., Generation of submicron dispersed aerosols in electrosprays. *Journal of Aerosol Science*, 1990, **21**, 673–676.
15. Ganan-Calvo, A. M., Davila, J. and Barrero, A., Current and droplet size in the electrospraying of liquids. *Journal of Aerosol Science*, 1997, **28**, 249–275.
16. Hartman, R. P. A., Marijnissen, J. C. M. and Scarlett, B., Electrohydrodynamic atomization in the cone-jet mode: a physical model of liquid cone and jet. *Journal of Aerosol Science*, 1997, **28**, S527–S528.
17. Hartman, R. P. A., Borra, J-P, Brunner, D.J., Marijnissen, J.C.M. and Scarlett, B., The evolution of electrohydrodynamic sprays produced in the cone-jet mode: a physical model. *Journal of Electrostatics*, 1999, **47**, 143–170.

18. Hartman, R. P. A., Brunner, D. J., Camelot, D. M. A., Marijnissen, J. C. M. and Scarlett, B., Electrohydrodynamic atomization in the cone-jet mode: physical modelling of the liquid cone and jet. *Journal of Aerosol Science*, 1999, **30**, 823–849.
19. Hartman, R. P. A., Brunner, D. J., Camelot, D. M. A., Marijnissen, J. C. M. and Scarlett, B., Jet break-up in the electrohydrodynamic atomization in the cone-jet mode. *Journal of Aerosol Science*, 2000, **31**, 65–95.
20. Jayasinghe, S. N. and Edirisinghe, M. J., Effect of viscosity on the size of relics produced by electrostatic atomization. *Journal of Aerosol Science*, 2002, **33**, 1379–1388.
21. Rosell-Llompart, J. and Fernandez de la Mora, J., Generation of monodisperse droplets 0.3 to 4μm in diameter from electrified cone-jets of highly conducting and viscous liquids. *Journal of Aerosol Science*, 1994, **25**, 1093–1119.
22. Jayasinghe, S. N., Edirisinghe, M. J. and De Wilde, T., A novel ceramic printing technique based on electrostatic atomization of a suspension. *Journal of Materials Research Innovations*, 2002, **6**, 92–95.
23. Balachandran, W., Miao, P. and Xiao, P., Electrospray of fine droplets of ceramic suspensions for thin-film preparation. *Journal of Electrostatics*, 2001, **50**, 249–263.